

Bose-Einstein condensation in inhomogeneous Josephson arrays

R. Burioni ^{1,2}, D. Cassi ^{1,2}, I. Meccoli ^{1,2}, M. Rasetti ^{1,4}, S. Regina ^{1,2}, P. Sodano ^{1,3}, A. Vezzani ^{1,2}

¹ *Istituto Nazionale Fisica della Materia (INFN)*

² *Dipartimento di Fisica, Università di Parma, Italy*

³ *Dipartimento di Fisica, Università di Perugia, Italy*

⁴ *Dipartimento di Fisica, Politecnico di Torino, Italy*

We show that spatial Bose-Einstein condensation of non-interacting bosons occurs in dimension $d < 2$ over discrete structures with inhomogeneous topology and with no need of external confining potentials. Josephson junction arrays provide a physical realization of this mechanism. The topological origin of the phenomenon may open the way to the engineering of quantum devices based on Bose-Einstein condensation. The comb array, which embodies all the relevant features of this effect, is studied in detail.

PACS numbers: 03.75.Fi, 85.25.Cp, 74.80.-g

The recent impressive experimental demonstration of Bose-Einstein Condensation (BEC) [1] has stimulated a new wealth of theoretical work aimed to better understanding its basic mechanisms [2] and, possibly, to exploit its consequences for the engineering of quantum devices.

It is well known [3] that for an ideal gas of Bose particles BEC does not occur in dimension $d \leq 2$, and an "ad hoc" external confining potential is needed to reach the required density of states. The same is true for free bosons living on regular periodic lattices, while the result cannot be extended to more general discrete structures lacking translational invariance.

In the following we shall prove that even for $d < 2$ [4] non-interacting bosons may lead to Bose-Einstein condensation into a single non-degenerate state, provided one resorts to a suitable discrete non-homogeneous support structure: indeed, when the bosonic kinetic degrees of freedom do not depend on metric features only, the particles may feel a sort of effective interaction due to topology. The proposed mechanism for BEC in lower dimensional systems is then a pure effect of the structure of the ambient space and avoids as well the need of resorting to external random potentials as the ones investigated by Huang in [2]; this is a very desirable feature in view of engineering real quantum devices.

In practice, the behavior of free bosons over generic discrete structures is made experimentally accessible through the realization of suitable arrays of Josephson junctions. The latter are devices that can be engineered in such a way as to realize a variety of non-homogeneous patterns. We shall show indeed that classical Josephson junction arrays arranged in a non-homogeneous geometry - not even necessarily planar - provide an example of the proposed mechanism for BEC, leading to a single state spatial condensation.

Theoretical studies of Josephson junction arrays are based on the short-range Bose-Hubbard model, since the phase diagram of Josephson junction arrays may be derived [5] from an Hamiltonian describing bosons with re-

pulsive interactions over a lattice. In $d = 1$ the phase diagram has been studied by analytical [6] and quantum Monte Carlo methods [7]; experimentally, Josephson junction arrays are used to study interacting bosons in one dimension. For a generic array the corresponding Hamiltonian is given by

$$H^{BH} = U \sum_i n_i^2 + \sum_{ij} A_{ij} \left(V n_i n_j - J (a_i^\dagger a_j + a_j^\dagger a_i) \right),$$

where A_{ij} is the adjacency matrix: $A_{ij} = 1$ if the sites i and j are nearest neighbors and $A_{ij} = 0$ otherwise; a_i^\dagger creates a boson at site i and $n_i \equiv a_i^\dagger a_i$. The phase diagram structure reflects the competition between the boson kinetic energy (hopping, favouring boson mobility) and repulsive interaction (Coulomb, working so as to suppress dynamics). In a realistic experimental setup [8], the parameters U and V depend on the ratio between the intergrain capacitance C and the gate capacitance C_0 , while the parameter J describes Cooper pair hopping. Josephson junction arrays allow for a good experimental control of C/C_0 and J , which can also be varied over a wide range. For $U \gg J, V$, and for bipartite arrays, Hamiltonian H^{BH} maps onto the quantum spin- $\frac{1}{2}$ XXZ model [9]. On the other hand, in the weak coupling limit ("classical" Josephson junctions) $U, V \ll J$, realizable when $C/C_0 \rightarrow 0$, the hopping term dominates the physical behaviour of the system, which is then described by the tight-binding Hamiltonian

$$H = -t \sum_{ij} A_{ij} a_i^\dagger a_j, \quad (1)$$

where t is an effective hopping parameter which accounts for a renormalization of the Josephson coupling J . For a non translation-invariant geometry of the array the tight-binding model, which describes "free" bosons over a regular lattice, cannot any longer be interpreted as representing non-interacting particles, just due to the ambient graph topology. We shall show the dramatic effect

of topology already on the simple graph referred to as square comb [10,11]. This provides an explicit and remarkable example of topology-induced mechanism leading to a spatial Bose-Einstein condensation in low dimension.

The "square comb" is the graph made of N "fingers" of N sites represented in Fig. 1. whose total number of sites is N^2 . In the following the generic vertex i is labelled with the "coordinate" indices (x_i, y_i) , $i \in \mathbf{Z}_N$ (where the latter requirement is imposed to guarantee periodic boundary conditions).

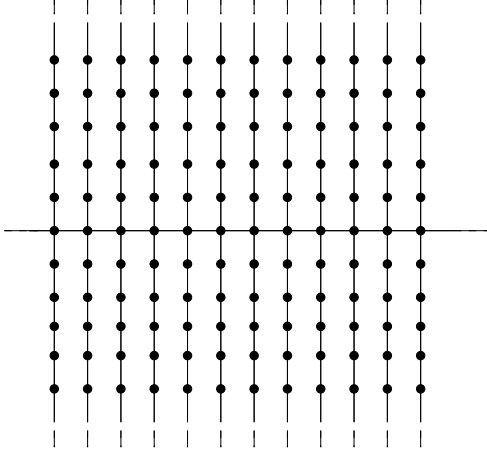


Fig. 1. The comb graph: the dots represent Josephson junctions and the links describe the topology of the array connections, with no reference to their embedding in real euclidean space.

The tight-binding model on the comb graph, is given by the Hamiltonian (1) with the adjacency matrix $A_{ij} = (\delta_{x_i, x_i+1} + \delta_{x_i, x_i-1}) \delta_{y_i, 0} \delta_{y_j, 0} + (\delta_{y_i, y_i+1} + \delta_{y_i, y_i-1}) \delta_{x_i, x_j}$. By exploiting the comb translation invariance in the direction of the backbone one can perform a Fourier Transform along the x direction obtaining a new Hamiltonian in the variables k_x :

$$H = -t \sum_{y, y'} \sum_{k_x} (\delta_{y, 0} \delta_{y, y'} \cos k_x + \bar{A}_{yy'}) a_{k_x, y}^\dagger a_{k_x, y'}, \quad (2)$$

where $k_x = 2\pi n/N$ and $n = 0, 1, \dots, N-1$ and $\bar{A}_{yy'}$ in the adjacency matrix for a linear chain (i.e. for each comb finger). The operator $a_{k_x, y}$ is given by: $a_{k_x, y} \equiv \sum_{x=1}^N e^{ik_x x} a_{(x, y)}$. Notice that (2) is the sum of N commuting Hamiltonians representing an one-dimensional tight-binding model with a local potential at site 0 of value: $-t \cos k_x$.

Each of the one-dimensional Hamiltonians appearing in eq. (2) can be diagonalized, in the thermodynamic limit. To do this one uses the property that for $y \geq 2$ and $y \leq -2$ the eigenvectors of $-(\delta_{y, 0} \delta_{y, y'} \cos k_x + \bar{A}_{yy'})$

are those of the Hamiltonian describing a free particle on the linear chain. Such eigenvectors are: $e^{\pm i k_y y}$ with eigenvalue $-2 \cos k_y$, $e^{\pm k_y y}$ with eigenvalue $-2 \cosh k_y$ and $(-1)^y e^{\pm k_y y}$ with eigenvalue $2 \cosh k_y$. If one requires that the eigenvalue equations hold also at sites $-1, 0, 1$ and that the eigenvectors are normalizable, one finds that the spectrum of the one dimensional problem is given by the isolated point $E = -2t \operatorname{sgn}(\cos k_x) \sqrt{1 + \cos^2 k_x}$ and by a continuous part $R_0 = \{E \mid |E| < 2t\}$ with a density of states given by $\rho_0(E) = (1/\pi)(N-1)(4t^2 - E^2)^{-1/2}$. From the spectra of the one dimensional problems corresponding to different values of k_x one obtains in the thermodynamic limit the density of states for the tight-binding Hamiltonian on the comb-graph (Fig. 2).

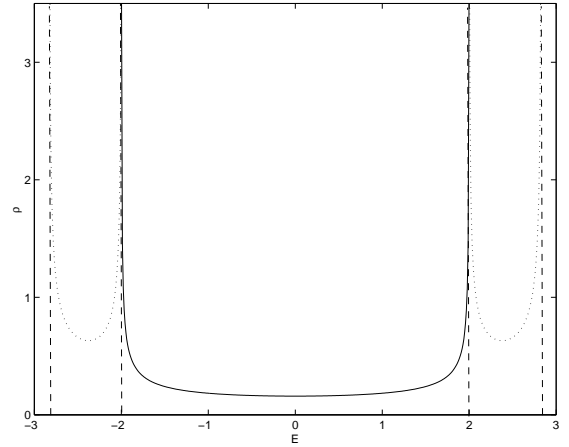


Fig. 2. The density of states of the Hamiltonian (1). The solid line indicates the continuous part of the spectrum ρ_0 , which is normalized to $N(N-1)$. The dot lines denote the sets of zero measure, the densities ρ_+ and ρ_- are normalized to N . The x -axis scale is in units of t .

The spectrum is made of three parts R_α , $\alpha = 0, \pm$: for $E \in R_0$ the density of states is given by:

$$\rho_0(E) = \frac{1}{\pi} N(N-1)(4t^2 - E^2)^{-1/2}.$$

Since $\int_{R_0} \rho_0(E) dE = N(N-1)$, in the thermodynamic limit, almost all the states, i.e. all the states apart a set of measure zero, belong to this region and $\lim_{N \rightarrow \infty} (\int_{R_0} \rho_0(E) dE)/N^2 = 1$. In the other two regions, $R_- = \{E \mid -\sqrt{8}t \leq E < -2t\}$ and $R_+ = \{E \mid 2t < E \leq \sqrt{8}t\}$, the density of states is given by:

$$\rho_-(E) = \rho_+(E) \equiv \rho_\pm(E) = hN \frac{|E|}{\sqrt{8t^2 - E^2} \sqrt{E^2 - 4t^2}},$$

where h must be chosen so that $\int_{R_- \cup R_+} \rho_\pm(E) dE = N$. There follows that in the thermodynamic limit only a subset of states of measure zero belongs

to these regions of the spectrum, in that one has $\lim_{N \rightarrow \infty} N^{-2} \int_{R_{\pm}} \rho_{\pm}(E) dE = 0$. The states with $E \in R_-$ play a fundamental role in the study of bosonic particles on comb structures. The lowest energy eigenstate of (1) (corresponding to $E_0 = -\sqrt{8}t$) is represented in Fig. 3. It is constant along the x direction for any fixed y , while along y it decreases exponentially with the distance from the backbone.

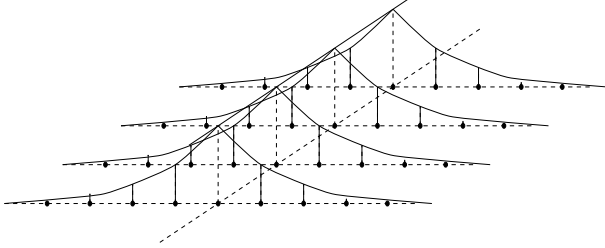


Fig. 3. The eigenvector corresponding to the lowest energy state. It is constant along the backbone direction and it decreases exponentially as $\exp(-\text{arcsch}(2) \cdot |x|)$ along the fingers.

If one introduces a finite bosonic filling f , i.e. if one fills the comb with fN^2 non interacting bosons, fixing the number of particles in the gran canonical partition function amounts to choosing the fugacity $z(N, \beta, f)$ as

$$f = N^{-2} \sum_{\alpha=-,0,+} \int_{R_{\alpha}} \frac{1}{z^{-1}e^{\beta E} - 1} \rho_{\alpha}(E) dE, \quad (3)$$

with $0 < z \leq e^{-\beta t \sqrt{8}}$. Since $\int_{R_+} (z^{-1}e^{\beta E} - 1)^{-1} \rho_+(E) dE < cN$, (c is a number independent of N and z), the third term of (3) vanishes in the thermodynamic limit. On the other hand, the first term can be positive and finite in the thermodynamic limit if $z(N, \beta, f) \rightarrow e^{-\beta t \sqrt{8}}$ when $N \rightarrow \infty$. Denoting by n_0 the fraction of particles with energy smaller than $-2t$, $n_0 = \lim_{N \rightarrow \infty} f^{-1} N^{-2} \int_{R_-} (z^{-1}(N)e^{\beta E} - 1)^{-1} \rho_-(E) dE$, one has that n_0 is a finite fraction of particle condensed in a subset of states of measure zero. In the thermodynamic limit, if β_c is the inverse temperature for which:

$$1 = \frac{1}{\pi f} \int_{R_0} \frac{dE}{(e^{\beta_c(E+t\sqrt{8})} - 1) \sqrt{4t^2 - E^2}},$$

one has that if $\beta \leq \beta_c$ there always exists a real and positive z solution of the equation

$$f = \frac{1}{\pi} \int_{R_0} \frac{dE}{(z^{-1}e^{\beta E} - 1) \sqrt{4t^2 - E^2}},$$

and $n_0 = 0$: there is no condensation. For $\beta > \beta_c$ one has $z = e^{-\beta t \sqrt{8}}$ and n_0 is given by

$$n_0 = 1 - \frac{1}{f\pi} \int_{R_0} \frac{dE}{(e^{\beta(E+t\sqrt{8})} - 1) \sqrt{4t^2 - E^2}}.$$

For $T < T_c \equiv (\beta_c)^{-1}$ there is Bose-Einstein condensation and in Fig. 4 we plot the fraction n_0 of particles in the condensate as a function of T for several values of the filling ($f = 0.5, 1, 2$). The points where the curves intersect the T-axis are the critical temperatures for the different fillings.

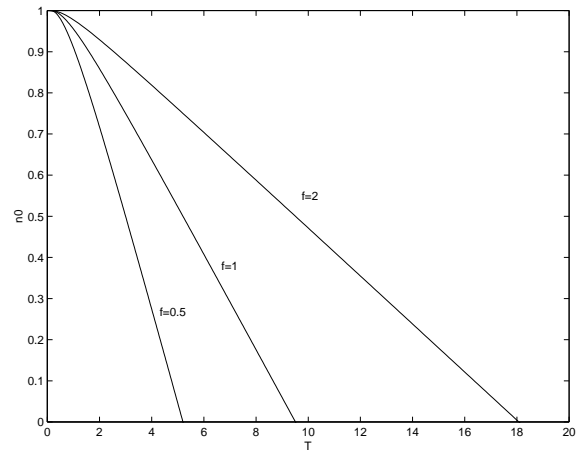


Fig. 4. The fraction n_0 of condensed particles as a function of the temperature T for different fillings $f = 0.5, 1, 2$.

For $T \rightarrow T_c^-$ the order parameter depends linearly on T since $n_0 \propto (T - T_c)$, and it is analytic in T for T close to T_c . The behaviour for $T \rightarrow 0$ is given by $n_0 \propto \sqrt{T} \exp(-(2\sqrt{2} - 2)t/KT)$. This is different from the customary Bose-Einstein condensation in a 3-d box, where $n_0 = 1 - (T/T_c)^{3/2}$. The critical temperature T_c exhibits the dependence on the filling f shown in Fig. 5, asymptotically ($f > 1$) linear and of the form $T_c \propto -(\ln f)^{-1}$ for $f \ll 1$. Both behaviours characterize a gapped system. The gap $(2\sqrt{2} - 2)t$ measures the difference between the ground state energy and the bottom of the spectral region R_0

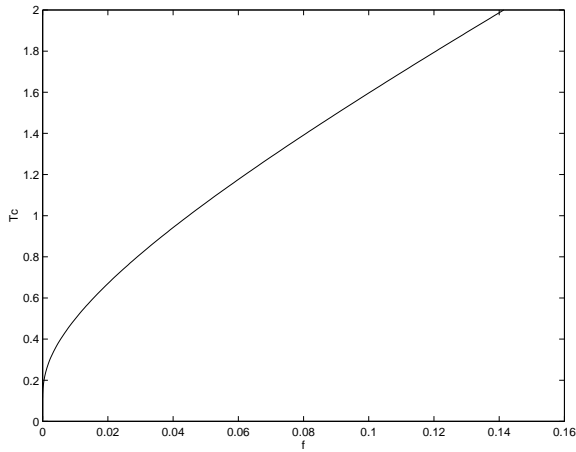


Fig. 5. The critical temperature T_c as a function of the filling f .

The average energy per particle

$$\langle E \rangle = -\sqrt{8}tn_0 + \frac{1}{f\pi} \int_{R_0} \frac{EdE}{(z^{-1}e^{\beta E} - 1)\sqrt{4t^2 - E^2}},$$

shows that all the particles in the condensate have energy $-t\sqrt{8}$, namely they are all in the ground state. Summarizing, in the thermodynamic limit and for $T > T_c$ almost all particles have energies between $-2t$ and $2t$ with the distribution $(z^{-1}e^{\beta E} - 1)^{-1}\rho_0(E)$, while for $T < T_c$ a finite fraction n_0 of particles is condensed in the state of lowest energy $E_0 = -\sqrt{8}t$. These particles occupy the inhomogeneous state described in Fig. 3, in which the sites closer to the backbone have larger filling than the farther ones.

In conclusion, we exhibited an explicit example (comb array) of Bose-Einstein condensation into a single state for non-interacting bosons, induced in dimension $d < 2$ by inhomogeneities without disorder and with no confining external potential in the discrete geometrical structure. The ensuing condensate shows deconfinement in one direction, i.e. along the comb backbone, and localization along the orthogonal direction; this is expected to lead to detectable singularities in the response functions.

The model Hamiltonian used is physically implementable by classical Josephson junction arrays, which it is possible to engineer in any desired geometric setting. Thus Bose-Einstein condensates arise as an intrinsic device feature, without need of fine-tuning any external control parameter.

Furthermore, it has been evidenced that a comb graph may emerge as a relevant geometrical structure if one consider a chain of classical Josephson junctions aligned along the direction of the backbone and interacting with a suitable external environment [12].

Finally, the same devices, as recently proposed [13], might lend themselves to be used for the realization of

BEC-based encoding and manipulation of quantum information [14]. The idea here is that because of the spontaneous symmetry breaking that characterizes it, a Bose-Einstein condensate should be quite naturally described by a non-linear quantum mechanics. Such non-linearity can be thought of as due just to the effective interaction of the bosons composing the condensate. In such a case the scenario recently described by Abrams and Lloyd [15] whereby non-linear quantum mechanics in the sense of Weinberg [16] implies polynomial time efficiency in dealing with **NP**-complete and **#P** complex computations would hold. It is intriguing that for the system presented here the relevant non-linearity, indeed present, is due to geometry and topology rather than to physical interactions.

-
- [1] F. Dalfovo, S. Giorgini, L.P. Pitaevskii, and S. Stringari, *Rev. Mod. Phys.* **71**, 463 (1999)
 - [2] A. Griffin, D.W. Snoke, and S. Stringari, eds.: *Bose-Einstein Condensation*, Cambridge University Press, Cambridge, 1995
 - [3] See e.g. K. Huang, *Statistical Mechanics*, Wiley, N. Y., 1963
 - [4] The dynamical dimensions of the graphs considered are strictly less than 2. See e.g. D. Cassi, and S. Regina, *Mod. Phys. Lett.* **B 11**, 997 (1997),
 - [5] M.P.A. Fisher, P.B. Weichman, G. Grinstein, and D.S. Fisher, *Phys. Rev.* **B 40**, 546 (1989), C. Bruder, R. Fazio, A. Kampf, A. van Otterlo, and G. Schön, *Phys. Sci.* **42**, 159 (1992) R.T. Scalettar, G.G. Batrouni, A.P. Kampf, and G.T. Zimanyi, *Phys. Rev.* **B 51**, 8467 (1995)
 - [6] J.K. Freeriks, and H. Monien, *Europhys. Lett.* **26**, 545 (1994); *Phys. Rev.* **B53**, 2691 (1996)
 - [7] G.G. Batrouni, R.T. Scalettar, and G.T. Zimanyi, *Phys. Rev. Lett.* **65**, 1765 (1990) P. Niyaz, R.T. Scalettar, C.Y. Fong, and G.G. Batrouni, *Phys. Rev.* **B 50**, 362 (1994)
 - [8] see, for example, A. van Oudenaarden, and J.E. Mooij, *Phys. Rev. Lett.* **76**, 4947 (1996)
 - [9] E. Altman, and A. Auerbach, *Phys. Rev. Lett.* **81**, 4484 (1998)
 - [10] D.C. Mattis, *Phys. Rev.* **B 20**, 349 (1979)
 - [11] G. Weiss, and S. Havlin, *Physica A* **134**, 474 (1986)
 - [12] A. Schmid, *J. Low Temp. Phys.* **49**, 609 (1982)
 - [13] D. Jaksch, H.-J. Briegel, J.I. Cirac, C.W. Gardiner, and P. Zoller, *Phys. Rev. Lett.* **82**, 1975 (1999)
 - [14] Yu Shi, *Quantum computation with Bose-Einstein condensation capable of solving NP-complete and #P problems*, Los Alamos E-print Archives, [quant-ph/9910073](http://arxiv.org/abs/quant-ph/9910073)
 - [15] D.S. Abram, and S. Lloyd, *Phys. Rev. Lett.* **81**, 3992 (1998)
 - [16] S. Weinberg, *Phys. Rev. Lett.* **62**, 485 (1989); *Ann. Phys. (N.Y.)* **194**, 336 (1989)